Nuclear Factor kappa B (NF-κB) Targeted Self-Assembled Nanoparticles Loaded with Methotrexate for Treatment of Rheumatoid Arthritis

Authors' Contribution:
Study Design A
Data Collection B
Statistical Analysis C
Data Interpretation D
Manuscript Preparation E
Literature Search F
Funds Collection G

AG 1 **Xiong Li**
FE 1 **Jin Qu**
B 1 **Tao Zhang**
BC 1 **Xi He**
D 2 **Ying Jiang**
E 2 **Jiangyan Chen**

1 Department of Sports Medicine, Xiangya Hospital Central South University, Changsha, Hunan, P.R. China
2 Department of Rheumatology, Xiangya Hospital Central South University, Changsha, Hunan, P.R. China

Corresponding Author: Xiong Li, e-mail: AlexanderuPerezxz@yahoo.com
Source of support: Departmental sources

Background: Nanotechnology is one of the most productive approaches for specifically delivering drug payloads to the region of interest to decrease nonspecific distribution and unwanted toxicities.

Material/Methods: We prepared glycol chitosan stearate self-assembled nanoparticles loaded with methotrexate (MTX) for NF-κB targeting in treatment of rheumatoid arthritis (RA). The nanoparticles were prepared using hydrophobic modification of glycol chitosan (GC) with steric acid (SA) and was characterized using IR. The efficiency of nanoparticles after their physiochemical characterization was measured *in vitro* and by *in vivo* studies in mice.

Results: The nanoparticles thus prepared were spherical in shape, 235 nm in diameter, and had negative zeta potential. The entrapment efficiency of MTX-GC-SA was more than 70%. The *in vitro* higher uptake of MTX-GC-SA in murine macrophage cells (RAW 264.7) was confirmed using confocal microscopy and FACS analysis. Systemic administration of MTX-GC-SA into collagen-induced arthritis (CIA) mice resulted in high accumulation in inflamed joints. The MTX-GS-SA revealed significantly better therapeutic efficacy against CIA mice compared to free MTX.

Conclusions: These findings highlight the potential of using this MTX-GC-SA nanoparticle formulation in suppressing inflammatory arthritis for effective treatment of RA.

MeSH Keywords: Arthritis, Rheumatoid • Methotrexate • Nanoparticles

Full-text PDF: https://www.medscimonit.com/abstract/index/idArt/917396

Background

Rheumatoid arthritis (RA) is a common autoimmune disease characterized by bone erosion, synovial joint inflammation, and cartilage deformation [1–3]. Impaired immunity and unfettered cytokine networks are the main characteristics associated with RA progression [4,5]. Macrophages (M1) are activated in inflamed joints by secreting huge amounts of inflammatory cytokines (TNF-α and IL-1β), leading to progression of RA [6,7]. In contrast, macrophages (M2) act as anti-inflammatory agents and actively participate in tissue repair. Therefore, converting the major M1 in arthritic joints to M2 may be an attractive treatment for RA [8,9]. NF-κB signaling is substantially involved in macrophage polarization, and inhibition of its signaling pathway can reverse the polarization from M1 in arthritic joints to M2. NF-κB is usually found in the cytoplasm as an inactive complex with an inhibitory kB protein. In RA conditions, the stimulation signals (TNF-α or IL-1b) degrade the inhibitor kB protein and release the NF-κB subunit to transfer to the nucleus, where it is converted into several pro-inflammatory signals. This ultimately leads to progressive cartilage destruction and serious RA progression [10]. Therefore, early diagnosis and treatment of RA is important [11,12]. There are few specific NF-κB inhibitors for blockage of inflammatory signals available for clinical use, and antirheumatic drugs are the main treatment of RA. Methotrexate (MTX) has been used as a first-line medicine against RA since the 1980s, and it is safe and effective [13,14]. However, RA patients require long-term use of MTX and many need to increase the dose for therapeutic effect, which prompts drug resistance and various severe adverse effects. Therefore, effective delivery of MTX to affected joints is a huge challenge [15]. There is a need to develop a novel delivery system to maintain a high concentration of MTX within the inflamed joints and reduce its adverse effects for treatment for RA. One way to avoid these problems is to capture MTX into naturally biodegradable polymers. The size of NPs in the nano range is expected to increase the aqueous solubility and stability.

Therefore, there is a need to develop a controlled and sustained drug delivery system suitable for these drugs to safely and effectively treat RA. Biodegradable polysaccharides like chitosan and its modifications like glycol chitosan (GC) have attractive features such as biocompatibility, biodegradability, and non-toxicity in the human body [16,17]. Stearic acid has a long acyl chain, provides a stronger interaction between the co-polymer and drug, and it allows for the release of the cargo in a sustained manner, which extends the duration of the therapeutic effect and targets the drug to specific sites, with reduced drug-related toxicity. Sodium alginate (SA), a natural polysaccharide, induces pro-inflammatory cytokine release and chemokines through macrophage activation.

In this study, we developed ion-cross-linked polymer NPs made by the interaction between oppositely charged polymers, which are amphiphilic in nature. This amphiphilic copolymerization has been shown to be an excellent drug carrier system. NPs can improve anti-inflammatory action with site-specific distribution. In the present study, we evaluated the hemocompatibility and cytotoxicity of the prepared MTX-GC-SA and compared it with blank NPs. We also evaluated the internalization of target cell and inhibition of NF-κB transcription, which resulted in anti-inflammatory property with controlled doses of MTX. These findings show the potential for effective treatment of RA using this novel MTX-GC-SA nanoparticle formulation.

Material and Methods

MTX, sodium alginate, glycol chitosan (GC, Mw 90 KD, 82.7% degree of deacetylation), stearic acid, [1-ethyl-3 (dimethylamino) propyl] carbodiimide hydrochloride (EDC), sodium azide-fluorecin isothiocyanate (FITC), fetal bovine serum (FBS), phosphate-buffered saline solution (PBS), and 3-(4, 5-Dimethylthiazol-2-yl)-2, 5-diphenyltetrazolium bromide (MTT) reagents and chemicals were obtained from Sigma-Aldrich, USA. The reagents used in the experiments were of analytical grade.

Synthesis of GC-Co-polymer

GC-Co-polymer was prepared using the EDC coupling process as described in previous reports [18]. Briefly, stearic acid (SA) and EDC (1: 1.2 ratio) were dissolved in ethanol (10 ml) and then vortexed to obtain a clear solution labelled as solution A, which was added drop-wise into 0.03 g/ml of GC aqueous solution with continuous stirring at room temperature. After 24 h, GC-SA was separated from unreacted solution by dissolving in dichloromethane. The solution was separated and then lyophilized in a freeze dryer to collect the GC-SA.

Preparation of MTX-GC-SA

The MTX-GC-SA was prepared by the counter-ion induced gellification with slight modification. Briefly, 10 ml (1% w/v) of sodium alginate solution (SA) was mixed with calcium chloride (1 mM, 1 ml) as a cross-linking agent, containing MTX (0.03% w/v) under constant magnetic stirring at 600 rpm. GC solution (2 mL, 2% w/v, pH 4.6) was added drop-wise to the above dispersion with constant stirring for 30 min, followed by probe sonication (25 W for 5 min) and the prepared NPs were kept at room temperature overnight. The MTX-GC-SA was collected by centrifugation (10 000 rpm for 1 h) and washed with distilled water, and the obtained pellets were dried by lyophilization to form MTX-GC-SA. In the absence of MTX, blank NPs were collected following the same procedure. Nile red-tagged

GC-SA particles were prepared by incubating the particles with an adequate amount of Nile red solution.

Characterization of MTX-GC-SA

The MTX-GC-SA was principally assessed by UV-Vis spectroscopy (Shimadzu, Japan) followed by transmission electron microscopy (TEM). The particle size and the size distribution, including charge on the particles, were measured, and the MTX-GC-SA was evaluated using a Malvern Zetasizer at 25ºC. All measurements were performed in triplicate. The sample was examined for the morphological characterization of MTX-GC-SA using TEM (JEM 2100 LaB6, JEOL, and Japan) and scanning electron microscopy (SEM, JSM-6700F).

% Entrapment efficiency (% EE) and% loading efficiency

% EE was determined in the sample by centrifugation of MTX-GC-SA at 10 000 rpm for 1 h. The resultant supernatant was collected as free drug and pellets as entrapped drug. The pellets were reconstituted and analyzed by UV for MTX content.

The total amount of MTX was the drug loading, and%EE was determined as follows:

$$EE(\%) = \frac{W1 - W2}{W2} \times 100\%$$

The% loading efficiency was calculated as follows:

$$LE(\%) = \frac{W1 - W2}{W3} \times 100\%$$

Where, W_1=weight of total drug, W_2=weight of un-entrapped drug and W_3=weight of nanoparticles.

In vitro release study

Briefly, MTX-GC-SA (equivalent of 5 mg MTX), blank NPs, and control release were carried out using a dialysis membrane. MTX-GC-SA blank NPs and control were filled in different dialysis bags containing 1% v/v of Tween 80 in phosphate-buffered saline, and suspended in a dissolution apparatus USP type II containing 500 ml of PBS with 1% Tween 80 at 37ºC and 100 rpm. At fixed time points (30 min, 1 h, 2 h, 4 h, 6 h, 8 h, 12 h, 18 h, 24 h, and 48 h), 1 ml was taken as a sample for further analysis and the same amount of fresh medium was added to maintain a strict sink condition [19].

Haemolytic study

The hemocompatibility assay study was performed in human blood collected from a volunteer using a previously reported method [20]. The human blood was collected in heparinized vials. The red blood cells (RBCs) were collected by centrifugation (1200 rpm for 10 min) and re-suspended in PBS at pH 7.4. The solution (0.5 mL) was dispersed with 1 mL NPs at pre-determined concentrations (5, 10, and 15 µg/mL) and kept for 1 h at 37°C. The solutions collected were centrifuged for 6 min at 1000 rpm. The absorbance of samples was measured using an ELISA plate reader at 480 nm. Triton-X and PBS were used as positive and negative control, respectively. The percent (%) hemolysis was calculated by the following equation:

$$Hemolysis(\%) = \frac{Absorbance\ samples - Absorbance\ negative}{Absorbance\ positive - Absorbance\ negative} \times 100\%$$

Qualitative and quantitative estimation of cellular localization in RAW 264.7 cells

Confocal microscopy and FACS were used for quantitative and qualitative analysis, respectively, of MTX-GC-SA internalization in cells. The RAW 264.7 cells were used for the cellular localization studies and were cultured in RPMI medium containing 10% (v/v) FBS with 1% penicillin-streptomycin solution. RAW 264.7 cells with a density of 1×10^6 cells/well were plated into 6-well culture plates and incubated for 24 h. Subsequently, the cells were gently washed and treated with Nile red-tagged MTX-GC-SA and free Nile red for 4 h. The Nile red concentration was measured using a fluorometer.

For confocal studies, the treated cells were fixed with ice cold methanol after the treatment and subsequently washed and stained with DAPI to stain the nucleus. The localization of the NPs within the cells was detected using a confocal microscope (Nikon Instruments, Inc., Japan). All experiments were performed in triplicate.

For FACS studies, the treated cells were collected using trypsin, and the fluorescence generated was analyzed using a FACS machine (BD Biosciences FACS Calibur flow cytometer).

Cytotoxicity studies

The cellular cytotoxicity of the prepared MTX-GC-SA were examined and compared with blank NPs and plain MTX. The assessment was carried out by MTT assay on C28/I2 cells [21]. C28/I2 cells were cultured as described above and incubated. To conduct the MTT studies, 5000 cells were seeded for 24 h in 96-well plates. NPs were added at equivalent concentrations of MTX (5 µg/ml, 10 µg/ml, and 15 µg/ml) to the plated cells and kept in the incubator for 24 h. Subsequently, the treated cells were washed and 20 µl MTT solution was added to each well. Following 4-h treatment with MTT reagent, 100 µl of formazan crystal solubilizing agent was added and the optical density of the plate was measured at 570 nm with

a microplate reader. The effective concentration of MTX-GC-SA was calculated using the IC50 value.

In vivo arthritis animal model and therapeutic efficacy of MTX-GC-SA

The animal experiments carried out were preapproved by the Ethics Committee of Xiangya Hospital of Central South University, Changsha, Hunan. Six-week-old male Wistar mice were placed in standard laboratory conditions. Arthritis in the mice were induced by the established method of complete Freund's adjuvant (CFA) (100 µl) via an intradermal injection in the hind paw of animals in each group, and special care was taken during the experiment to prevent animal suffering [22].

When the arthritis was developed, which took about 5 weeks, the mice were divided into 4 groups, with 5 animals in each group. Group I was a control group (without treatment), Group II was administered PBS, Group III was administered free MTX, and Group IV was administered MTX-GC-SA (equivalent to 0.5 mg/kg MTX). The treatment was given every third day through intravenous injection. The arthritis score and the paw thickness were determined on different days. At the end of the study, blood was collected from each group and the level of IL-1β and TNF-α cytokines were measured by ELISA assay according to the kit instructions.

Statistical analysis

The results were analyzed using ANOVA. P<0.05 was considered as statistically significant.

Results and Discussion

Formulation and characterization of MTX-GC-SA

We used an amphiphilic co-polymer, which is a mixture of hydrophilic and hydrophobic cores. The scheme is illustrated in Figure 1, which has been characterized by IR studies, as shown in Figure 2. The IR spectrum shows the functional groups of GC-SA, indicating the successful hydrophobic modification of GC polymer. The broad peak at 3380 cm^{-1} shows the vibration of O-H stretching, which might have overlapped with the N-H stretching of amine. The next 2 peaks, arising near 2930 cm^{-1}, represent the stretching vibration of C-H. The peak arising near 1600 cm^{-1} confirms the amide stretch due to the formation of GC-SA polymer. This amphiphilic co-polymer was found to have superior mechanical strength with enhanced sustained release pattern and less toxicity. In addition, they have the ability to induce cytokine formation by NF-κB signaling. The counter-ion induced gellification process was used to prepare MTX-GC-SA. The size and particle distribution of MTX-GC-SA used
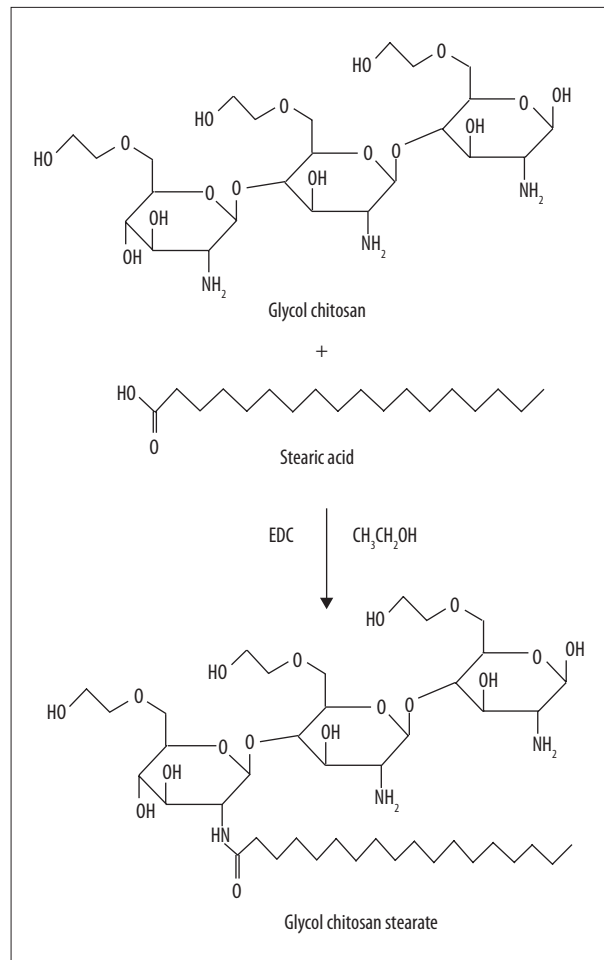
Figure 1. Synthesis scheme of the glycol chitosan stearate.
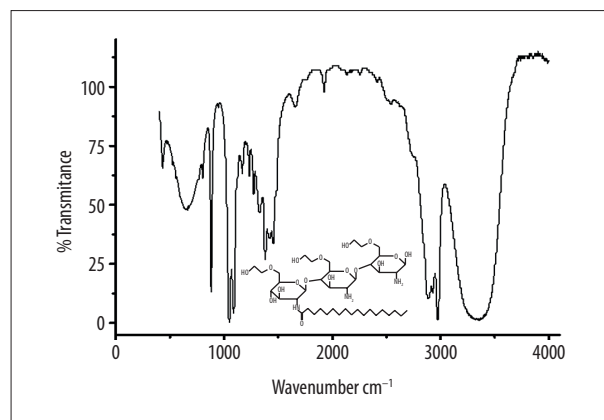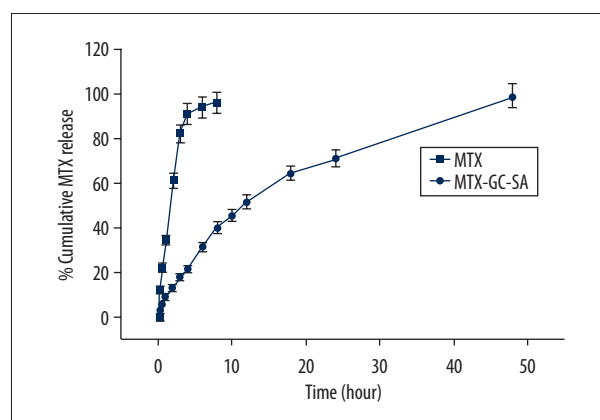

Figure 2. IR spectra showing the characteristic peaks of glycol chitosan stearate.
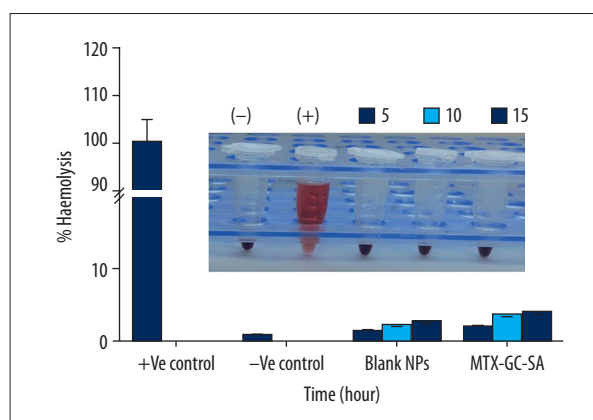
in our study was characterized by DLS. The results of mean size and particle distribution, zeta potential, and% entrapment efficiency (EE) of MTX-GC-SA are summarized in Table 1. The MTX-GC-SA particle size was 235.8±2.67 nm, with poly dispersity (PDI) of MTX-GC-SA (0.149±0.017), which was further

Table 1. Characterization of MTX-GC-SA.

| S. No.	Formulation	Size (nm)	Poly dispersity index (PDI)	Zeta potential (mV)	% entrapment efficiency
1	MTX-GC-SA	235.8±2.67	0.149±0.017	−20.4±1.13	73.4±3.7
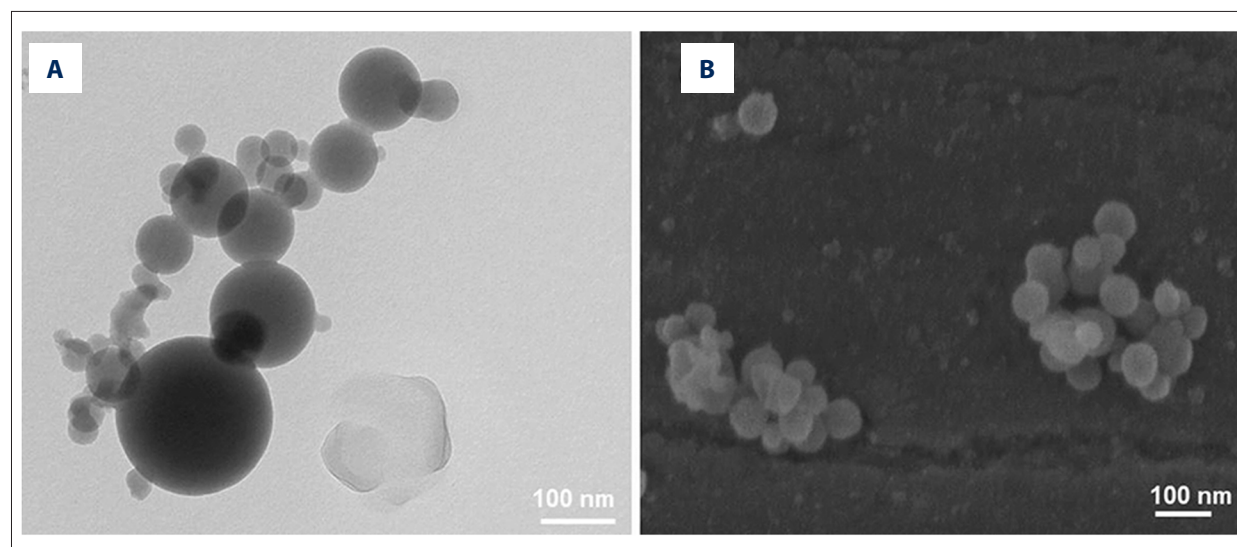
Figure 3. (**A**) Transmission electron microscopy image of MTX-GC-SA: (**B**) Scanning electron microscopy image of MTX-GC-SA.

Figure 4. *In vitro* MTX release from blank NPs and MTX-GC-SA in pH 7.4 PBS for 48 h.

Figure 5. Hemolysis study results showing safety of MTX-GC-SA in comparison with other groups.

confirmed by the zeta potential. The zeta potential of MTX-GC-SA was −20.4±1.13 mV. The MTX-GC-SA showed a negative zeta potential because the complete mask of SA is anionic polymer, which has good stability and optimal drug delivery [23]. The%EE in MTX-GC-SA was 73.4 ± 3.7, depending on the concentration of co-polymer used. The existence of MTX-GC-SA was also confirmed by TEM and SEM. Figure 3A shows that the morphology of the MTX-GC-SA was approximately spherical and relatively the same size, without any aggregation, and Figure 3B shows an SEM image of MTX-GC-SA.

In vitro release study

The *in vitro* release study of MTX from MTX-GC-SA and blank NPs was performed by using dialysis membrane (cut-off mol. wt. 12 KD) using Tween 80 to assist the release of drug in the solution. The *in vitro* release of MTX-GC-SA and blank NPs showed a properly controlled release profile. The release profiles of MTX from MTX-GC-SA and free MTX was compared and examined using HPLC. The quantity of drug released was 12.81% and 16.80% for MTX-GC-SA after 2 h at pH 7.4 and 37°C. This initial slow release in the MTX-GC-SA was due to
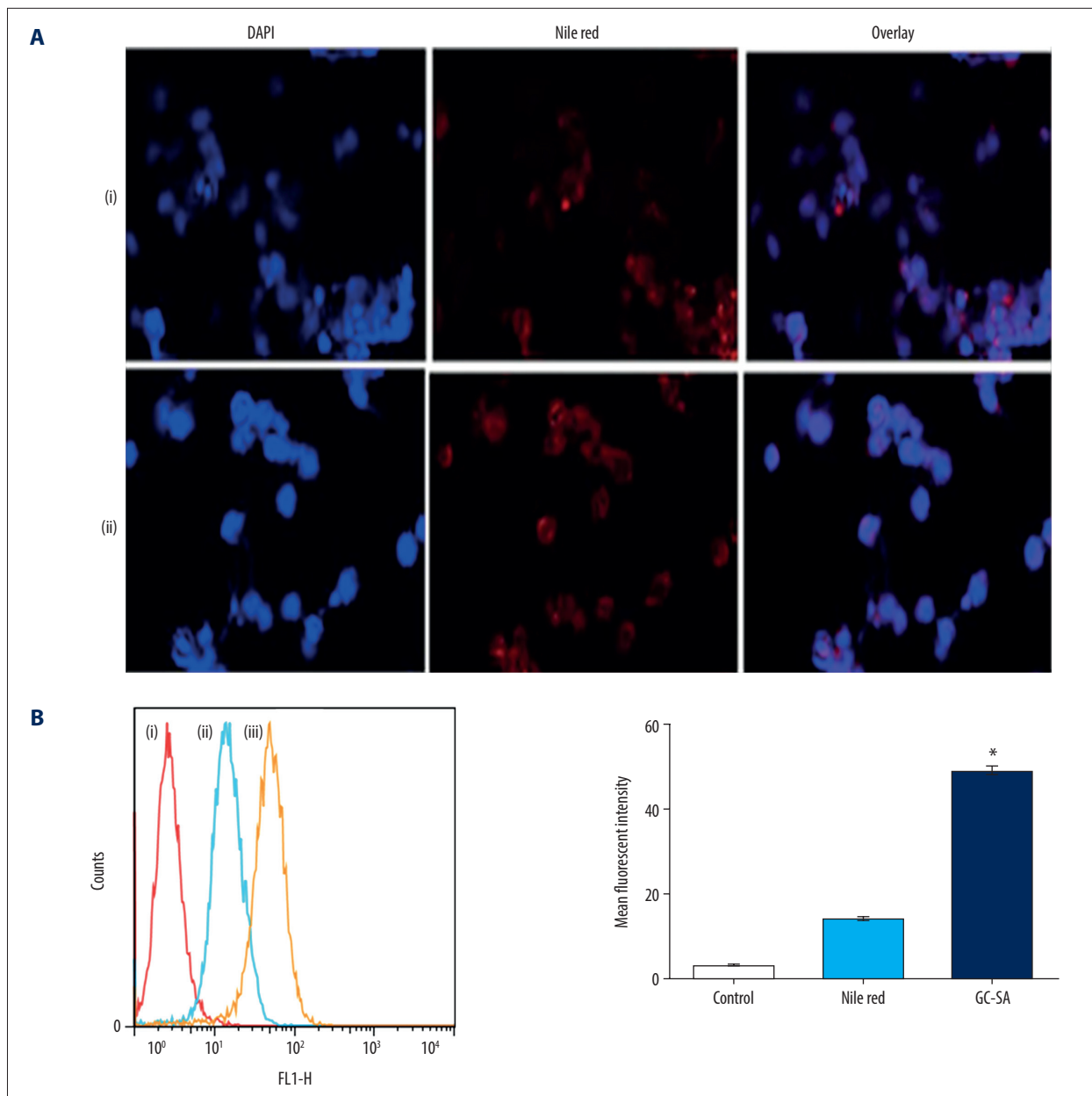
Figure 6. (**A**) Confocal fluorescence image of a single XY optical section of RAW 264.7 cells after uptake of (i) plain Nile red (ii) Nile red-labelled MTX-GC-SA. (**B**) FACS analysis in cells after the treatment: (i) without treatment (control), (ii) plain Nile red, and (iii) Nile red-labelled MTX-GC-SA (*p < 0.05 Nile red *vs.* Nile red-labelled MTX-GC-SA).

its steric repulsion characteristics, which makes it an effective delivery system because of the long circulation vector in drug delivery applications. After 18 h, the release rate of MTX was 64.1% from MTX-GC-SA, as illustrated in Figure 4. After 24 h, the release was 70.7% for MTX-GC-SA. The complete release of MTX from MTX-GC-SA was within 48 h. These data show that the NPs sustained the MTX release in the dissolution medium.

Haemolytic toxicity study

We performed a hemolysis toxicity study to assess the impairment of red blood cells caused by prepared NPs at different concentrations. The study was necessary to confirm erythrolytic lysis caused by different NPs. The hemocompatibility of MTX-GC-SA and blank NPs is displayed in Figure 5. These results clearly show that less than 5% hemolysis caused by MTX-GC-SA and blank NPs at the highest test concentrations provides favourable hemocompatibility. MTX-GC-SA and blank NPs
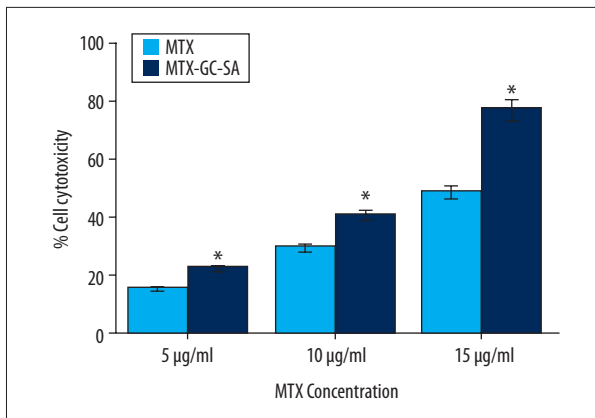
Figure 7. % cell cytotoxicity graph of effect of MTX and MTX-GC-SA on C28/I2 cells after 24-h exposure. MTX-GC-SA reveals significantly higher cytotoxicity in comparison with free MTX (* p<0.05)

have low protein binding and hemocompatibility, which confirmed their potential for therapeutic application.

Cellular localization

The intercellular uptake of NPs was determined using confocal imaging by fluorescent-labelled MTX-GC-SA and free Nile red. DAPI was colored blue, which served as a nucleus-staining dye, whereas red color showed Nile red-tagged NPs. The cellular internalization in macrophages under an inflammatory condition was assessed, in which cells were treated with lipopolysaccharide (LPS) to activate an inflammatory state [24]. Generally, LPS-activated macrophages are present in RA. MTX-GC-SA was clearly shown to be more internalized compared to blank NPs, as shown in Figure 6A. The FACS studies also revealed significantly (p<0.05) higher internalization of MTX-GC-SA in the cells as compared with control and plain Nile red,

as shown in Figure 6A. This result indicates that the prepared MTX-GC-SA was able to deliver MTX into the cytosol of the target cells by a passive mechanism [10,25], which may potentially inhibit NF-κB-based inflammatory activity.

Cytotoxicity studies

The MTT of C28/I2 cells was calculated after treatment with different concentrations of MTX from different NPs. As displayed in Figure 7, the cell viability of MTX-GC-SA and blank NPs at a concentration 15 μg mL-1 after 24-h incubation was 48% and 41%, respectively, whereas cells treated with plain drug had 76% cell viability. The calculated IC50 values for MTX and MTX-GC-SA were 15.46 μg/mL and 9.40 μg/mL, respectively. Moreover, the results suggest that the cytotoxicity caused by MTX-GC-SA in cells was significantly higher than in the free MTX group (p<0.05). This might be why MTX loaded in MTX-GC-SA was more susceptible in cells, via an endocytosis mechanism, as compared with plain MTX, as also revealed by cellular uptake studies. As a result, the redox balance was disturbed (the level of glutathione reduction was lower), and the signal cascade (NF-κB) was activated, which further aggravated the formation of cytokines in RA patients [26].

Therapeutic efficacy of MTX-GC-SA

Next, we measured the efficacy of the developed MTX-GC-SA in the arthritic mice. The results were compared with the control group, showing that the arthritis score continuously increased in the PBS group but not in the free MTX group. MTX-GC-SA significantly improved the arthritis scores. The paw thickness was also significantly lower in the MTX-GC-SA group mice compared to other groups, including the free MTX group. Statistical analysis showed that the arthritis score and paw thickness of mice treated with MTX-GC-SA were not significantly different
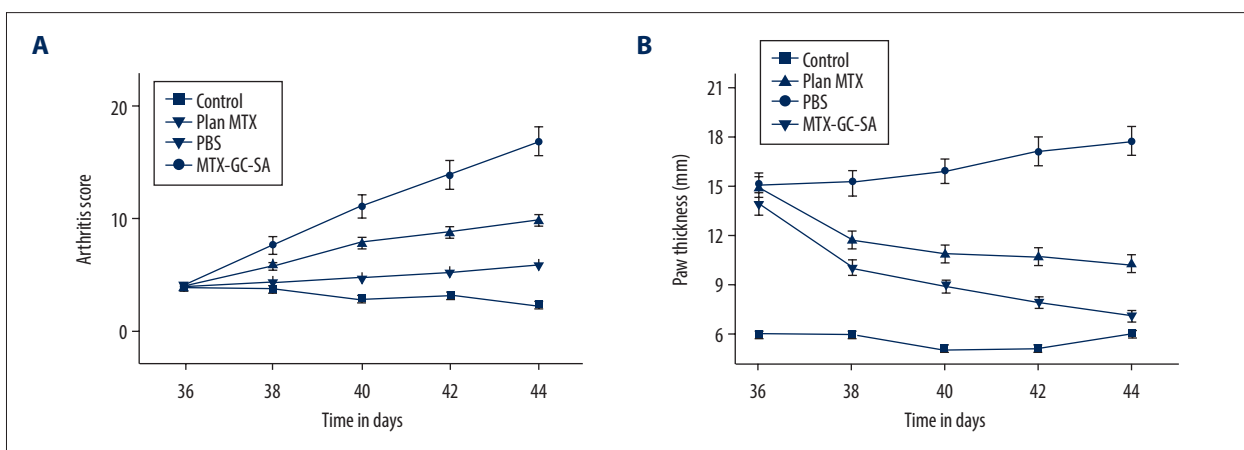
Figure 8. The therapeutic efficacy of MTX-GC-SA in arthritic mice: (**A**) arthritis score and (**B**) paw thickness. The arthritis score and paw thickness of mice treated with MTX-GC-SA was significantly less than the mice treated with free MTX and PBS (p<0.05 and p<0.01 respectively).
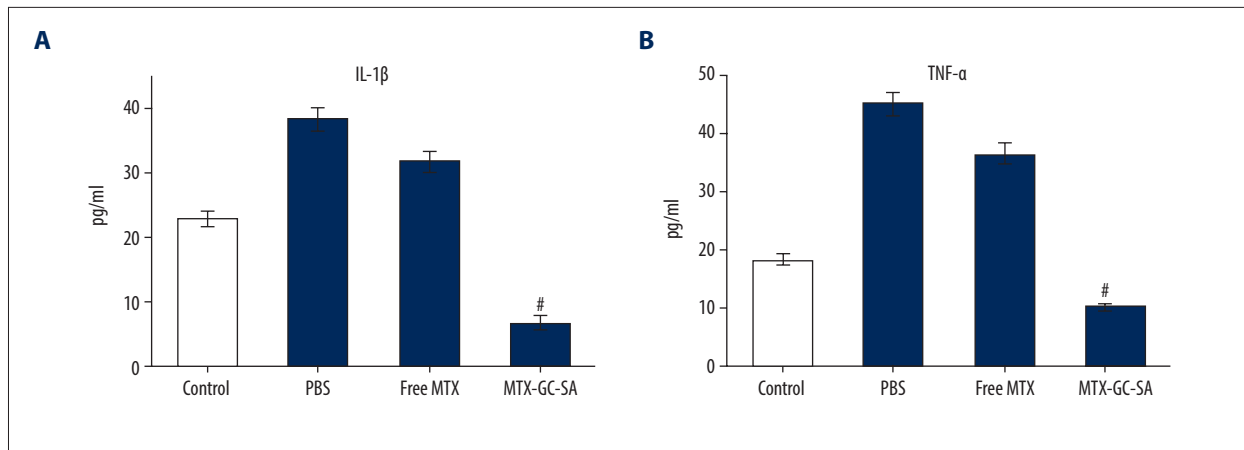
Figure 9. The level of pro-inflammatory cytokines in serum was analyzed: (**A**) IL-1β (**B**) TNF-α. The pro-inflammatory cytokines were significantly (p<0.05) decreased in the MTX-GC-SA group compared with the free MTX group.

from the control group. However, the arthritis score and paw thickness of mice treated with MTX-GC-SA were significantly less than in mice treated with free MTX or PBS (p<0.05 and p<0.01, respectively), possibly due to the accumulation of MTX-GC-SA in areas affected by arthritis (Figure 8A, 8B).

Serum levels of IL-1β and TNF-α considered an important indicators of RA progression, as further confirmed by the above results [27]. As seen in Figure 9A and 9B, free MTX and PBS showed higher levels of IL-1β and TNF-α, respectively, which are hallmarks of RA progression. The MTX-GC-SA-treated group had significantly lower levels of IL-1β and TNF-α than in the control group, suggesting an inhibitory effect on pro-inflammatory cytokine signals. These results show the significant decrease in pro-inflammatory cytokines in the MTX-GC-SA group compared with the free MTX group (p<0.05).

Conclusions

MTX-GC-SA is a novel and simple delivery system that shows better therapeutic activity than standard MTX. Its superiority may be due to the fact that MTX is easily encapsulated in the amphiphilic co-polymer of these NPs, which has a sustained release mode with polymer degradability. These results show that the developed formulations were engulfed by the cells and thus are also effective in localized treatment in mice. Studies agree regarding the effect of suppressing the NF-κB pathway and reducing the expression of pro-inflammatory cytokines. The present study clearly demonstrates that MTX-GC-SA is a biologically safe, cost effective, and superior method for achieving good scalability.

Conflict of interest

None.

References:

1. Darrieutort-Laffite C, Boutet MA, Chatelais M et al: IL-1β and TNFα promote monocyte viability through the induction of GM-CSF expression by rheumatoid arthritis synovial fibroblasts. Mediators Inflamm, 2014; 2014: 241840

2. McInnes IB, G Schett: The pathogenesis of rheumatoid arthritis. N Engl J Med, 2011; 365(23): 2205–19

3. Chen Y, Wang X, Yang M et al: miR-145-5p increases osteoclast numbers *in vitro* and aggravates bone erosion in collagen-induced arthritis by targeting osteoprotegerin. Med Sci Monit, 2018; 24: 5292–300

4. Firestein GS, McInnes IB: Immunopathogenesis of rheumatoid arthritis. Immunity, 2017; 46(2): 183–96

5. Guo Q, Wang Y, Xu D et al: Rheumatoid arthritis: Pathological mechanisms and modern pharmacologic therapies. Bone Res, 2018; 6: 15

6. Udalova IA, Mantovani A, Feldmann M: Macrophage heterogeneity in the context of rheumatoid arthritis. Nat Rev Rheumatol, 2016; 12(8): 472–85

7. Xia ZB, Yuan YJ, Zhang QH et al: Salvianolic acid B suppresses inflammatory mediator levels by downregulating NF-kappaB in a rat model of rheumatoid arthritis. Med Sci Monit, 2018; 24: 2524–32

8. Jain S, Tran TH, Amiji M: Macrophage repolarization with targeted alginate nanoparticles containing IL-10 plasmid DNA for the treatment of experimental arthritis. Biomaterials, 2015; 61: 162–77

9. Jang SE, Hyam SR, Han MJ et al: Lactobacillus brevis G-101 ameliorates colitis in mice by inhibiting NF-kappaB, MAPK and AKT pathways and by polarizing M1 macrophages to M2-like macrophages. J Appl Microbiol, 2013; 115(3): 888–96

10. Wang Q, Jiang H, Li Y et al: Targeting NF-κB signaling with polymeric hybrid micelles that co-deliver siRNA and dexamethasone for arthritis therapy. Biomaterials, 2017; 122: 10–22

11. Wang Q, Wang W, Zhang F et al: NEAT1/miR-181c regulates osteopontin (OPN)-mediated synoviocyte proliferation in osteoarthritis. J Cell Biochem, 2017; 118(11): 3775–84

12. Li S, Chen J-W, Xie X et al: Autophagy inhibitor regulates apoptosis and proliferation of synovial fibroblasts through the inhibition of PI3K/AKT pathway in collagen-induced arthritis rat model. Am J Transl Res, 2017; 9(5): 2065–76

13. Zhao J, Zhang X, Sun X et al: Dual-functional lipid polymeric hybrid pH-responsive nanoparticles decorated with cell penetrating peptide and folate for therapy against rheumatoid arthritis. Eur J Pharm Biopharm, 2018; 130: 39–47

14. Pincus T, Yazici Y, Sokka T et al: Methotrexate as the "anchor drug" for the treatment of early rheumatoid arthritis. Clin Exp Rheumatol, 2003; 21(5 Suppl. 31): S179–85

15. Khan ZA, Tripath R, Mishra B: Methotrexate: A detailed review on drug delivery and clinical aspects. Expert Opin Drug Deliv, 2012; 9(2): 151–69

16. Khatik R, Mishra R, Verma A et al: Colon-specific delivery of curcumin by exploiting Eudragit-decorated chitosan nanoparticles *in vitro* and *in vivo*. Journal of Nanoparticle Research, 2013; 15(9): 1893

17. Uchegbu IF, Sadiq L, Arastoo M et al: Quaternary ammonium palmitoyl glycol chitosan – a new polysoap for drug delivery. Int J Pharm, 2001; 224(1–2): 185–99

18. Gupta PK, Jaiswal AK, Asthana S et al: Self-assembled ionically sodium alginate cross-linked amphotericin B encapsulated glycol chitosan stearate nanoparticles: Applicability in better chemotherapy and non-toxic delivery in visceral leishmaniasis. Pharm Res, 2015; 32(5): 1727–40

19. Dwivedi P, Khatik R, Khandelwal K et al: Preparation and characterization of solid lipid nanoparticles of antimalarial drug arteether for oral administration. Journal of Biomaterials and Tissue Engineering, 2014; 4(2): 133–37

20. Khatik R, Dwivedi P, Shukla A et al: Development, characterization and toxicological evaluations of phospholipids complexes of curcumin for effective drug delivery in cancer chemotherapy. Drug Deliv, 2016; 23(3): 1067–78

21. Park JS, Yang HN, Jeon SY et al: The use of anti-COX2 siRNA coated onto PLGA nanoparticles loading dexamethasone in the treatment of rheumatoid arthritis. Biomaterials, 2012; 33(33): 8600–12

22. Newbould BB: Chemotherapy of arthritis induced in rats by mycobacterial adjuvant. Br J Pharmacol Chemother, 1963; 21: 127–36

23. Thu B, Bruheim P, Espevik T et al: Alginate polycation microcapsules. II. Some functional properties. Biomaterials, 1996; 17(11): 1069–79

24. Duan W, Li H: Combination of NF-κB targeted siRNA and methotrexate in a hybrid nanocarrier towards the effective treatment in rheumatoid arthritis. J Nanobiotechnology, 2018; 16(1): 58

25. King TJ, Georgiou KR, Cool JC et al: Methotrexate chemotherapy promotes osteoclast formation in the long bone of rats via increased pro-inflammatory cytokines and enhanced NF-kappaB activation. Am J Pathol, 2012; 181(1): 121–29

26. Fatima N, Faisal SM, Zubair S et al: Role of pro-inflammatory cytokines and biochemical markers in the pathogenesis of type 1 diabetes: Correlation with age and glycemic condition in diabetic human subjects. PLoS One, 2016; 11(8): e0161548

27. Charles P, Elliott MJ, Davis D et al: Regulation of cytokines, cytokine inhibitors, and acute-phase proteins following anti-TNF-alpha therapy in rheumatoid arthritis. J Immunol, 1999; 163(3): 1521–28